Dynamical Model for the Buoyancy-Driven Zigzag Motion of Oblate Bodies

Patricia Ern,[1,2] Frédéric Risso,[1,2] Pedro C. Fernandes,[1,2] and Jacques Magnaudet[1,2]
[1]*Université de Toulouse; INPT, UPS; IMFT (Institut de Mécanique des Fluides de Toulouse); Allée Camille Soula, F-31400 Toulouse, France*
[2]*CNRS, IMFT, F-31400 Toulouse, France*
(Received 2 October 2008; published 3 April 2009)

We describe a dynamical model that predicts the zigzag motion of disks and oblate spheroids moving freely in a viscous liquid over a continuous range of aspect ratios and Reynolds numbers. This model combines the generalized Kirchhoff equations to describe the linear and angular momentum balances for the fluid-body system with a dynamical model for the wake-induced force and torque that incorporates the main characteristics of the wake dynamics deduced from previous experimental observations. The resulting model is shown to be able to reproduce quantitatively the oscillatory paths measured experimentally.

DOI: 10.1103/PhysRevLett.102.134505 PACS numbers: 47.55.−t, 47.15.Tr, 47.27.ed, 47.55.dd

Bodies of different shapes, materials, or densities frequently select a periodic path when rising or falling freely in a fluid at rest under the action of buoyancy: a winged-seed undulating in air, a paper card tumbling during its fall, a bubble spiraling in water are examples of such periodic motions. This generic behavior results from the coupling between the motion of the body and that of the surrounding fluid: a body displacement induces a movement in the fluid, which in turn modifies the motion of the body through the hydrodynamic loads acting on it. However, there is at present no general theoretical framework that completely describes the evolution of these loads along a body's periodic path. More precisely, several empirical models specifically considered the case of a two-dimensional plate [1–4] or that of a bubble [5]. Nevertheless, such models are unable to describe the variety of periodic motions observed when the control parameters of the problem are varied continuously. The goal of the present Letter is to elaborate such a model for the case of disks of various aspect ratios and, more generally, of ''oblate'' axisymmetric bodies, by combining the findings and scaling laws provided by a recent series of experiments. These experiments [6–8] revealed that disks (of diameter d and thickness h) of variable aspect ratio $2 < \chi = \frac{d}{h} < 10$ rising with a Reynolds number in the range $100 < \mathrm{Re} = \frac{Vd}{\nu} < 330$ (V being the body vertical velocity and ν the liquid kinematic viscosity) exhibit a wide range of zigzagging styles on almost two-dimensional paths: the oscillations of the orientation and those of the velocity are nearly in phase for thick bodies ($\chi \leq 3$) (the body axis is almost aligned with the tangent to the path, as also happens in the case of a bubble), whereas they are more than $\pi/2$ out-of-phase for thin bodies ($\chi \geq 8$) (the body seems to slide along the path with its midplane almost aligned with the tangent to the path, as is also observed for a two-dimensional plate or a dead leaf). This change occurs gradually when χ increases and was also observed for oblate spheroids [6].

All modern models for this class of buoyancy-driven motions are based on the generalized Kirchhoff equations that describe the linear and angular momentum balances for the fluid-body system [9–11]. In these equations, the body inertia supplemented by a certain added inertia of the surrounding fluid is balanced by the buoyancy loads and the vortical loads resulting from the existence of a wake past the body, owing to the vorticity generated at the body surface. These loads are the key issue of the modeling problem. Previous investigations [1–4] assumed that the vortical loads are only a function of the body degrees of freedom. Inspired from the classical relations established for a lifting body held fixed in a steady uniform stream (in particular the well-known Kutta-Joukowski condition), these models consider that the vortical loads are linear or quadratic functions of the translational and/or angular velocity components of the body. Obviously, the time-dependent motions they predict result directly from the mathematical properties of the underlying equations. In particular, the basic assumption made in these models forces the phase lag between the oscillations of the body velocity and those of its inclination to be locked, thus preventing these models from a generalization that would allow them to reproduce the variety of zigzag styles observed experimentally in [7]. Since this phase difference is directly related to the wake dynamics through the evolution of the vortical loads [12], a different angle of attack is to introduce a dynamical model for the vortical loads that takes into account the main characteristics of the wake dynamics. This is the approach we follow in this Letter. This approach is grounded on earlier works aimed at describing the wake dynamics about fixed bodies and the associated transitions through low-order models (see for instance [13]), an approach also applied successfully within the framework of fluid-structure interactions (see for instance [14]).

Let x be the direction along the body symmetry axis and (y, z) two orthogonal directions in the perpendicular plane with the z axis horizontal and the body moving in the vertical plane (x, y). The body velocity components in this plane are (u, v) and $r = \frac{d\theta}{dt}$ is the rotation rate of the body about the z axis, θ being the angle between the vertical and the x axis. The generalized Kirchhoff equations written componentwise are

$$S(\mathrm{M} + \mathrm{A})\frac{du}{dt} - S(\mathrm{M} + \mathrm{B})vr = \mathrm{F}_\omega^x + \cos\theta, \quad (1)$$

$$S(\mathrm{M} + \mathrm{B})\frac{dv}{dt} + S(\mathrm{M} + \mathrm{A})ur = \mathrm{F}_\omega^y - \sin\theta, \quad (2)$$

$$S^2(\mathrm{MJ} + \mathrm{Q})\frac{dr}{dt} - (\mathrm{A} - \mathrm{B})uv = \Gamma_\omega^z. \quad (3)$$

with $\mathrm{M} = \frac{\rho_s}{\chi\rho_f}$ (in what follows, the ratio of the body-to-fluid densities ρ_s/ρ_f, is set to a fixed value very close to 1, to mimic experimental conditions in [7]). These equations have been normalized using the scales $l_0 = d$, $u_0 = (\frac{|\rho_s - \rho_f|}{\rho_f} gh)^{1/2}$, $f_0 = \rho_f u_0^2 \pi d^2$, for the length, velocity and force, respectively, g denoting gravity. These scales generate the inertial time scale $t_0 = l_0/u_0$, set by the mean rise motion. Using instead the time scale $t_\omega = \omega^{-1}$, where ω is the angular frequency of the body oscillatory motion introduces the Strouhal number $S = t_0/t_\omega$. Experiments [7] indicated that S evolves according to $S \approx 2\pi \times 0.085\chi^{1/2}(1 + 0.047(\mathrm{Re}^* - \mathrm{Re}_c^*))$, with $\mathrm{Re}_c^* = 72$. The modified Reynolds number Re^* is built on the maximum of the reverse velocity in the recirculating region of the wake and characterizes the strength of wake effects. Based on values determined for stationary wakes, it was found in [7] that Re^* is linked to Re through the simple empirical relation $\mathrm{Re}^* = 0.62\mathrm{Re}\chi/(1 + \chi)$. The left-hand side of (1)–(3) contains the inertia terms associated with the body (J is the dimensionless moment of inertia of the body about the z axis), and those due to the fluid set in motion instantaneously by a translational or a rotational acceleration of the body (characterized by the added-mass coefficients A, B, and Q) [12]. On the right-hand side, the sinusoidal functions of θ are the components of the buoyancy force and F_ω^x and F_ω^y stand for the components of the vortical force $\mathbf{F}_\omega$ along the x and y directions, respectively, while Γ_ω^z is the component of the vortical torque $\mathbf{\Gamma}_\omega$ along the z direction.

The experimental results revealed that the body dynamics (kinematics) can be split into the predominant contribution of steady axial drag (resp. constant axial velocity) and a smaller-amplitude contribution provided by the oscillatory transverse forces and torques (transverse velocity and angular rotation). Equation (1) mainly corresponds to an equilibrium between the buoyancy force and a constant drag force, $\mathrm{F}_\omega^x \simeq -\cos\theta \simeq -1$, which results in the constant axial velocity, $u \simeq 1.35\text{–}3.5 \times 10^{-3}(\mathrm{Re}^* - \mathrm{Re}_c^*)$ [12]. The oscillations of the transverse velocity v and of the inclination angle θ are driven by the vortical loads F_ω^y and Γ_ω^z, whose oscillations are a direct consequence of the vortex shedding process. We therefore introduce an equation to model the evolution of F_ω^y, based on two physical ingredients characterizing the wake dynamics. First, the saturated amplitude of the oscillations of the transverse force is proportional to the quantity $(\mathrm{Re}^* - \mathrm{Re}_c^*)^{1/2}$, which is representative of the intensity of the vortices in the body near-wake [12]. Second, the time required to approach the limit cycle of regular oscillations once the body is released from rest scales with the inertial time scale t_0 set by the mean rise motion. Actually, this time scale was found to govern the leading-order evolution of the vortex structure in the body wake [8] and can therefore be expected to control the time required by the wake to set a periodic shedding of vortices in phase with the body motion. A simple model accounting for both these properties can be written in the form of an envelope equation for the amplitude F of the transverse vortical force F_ω^y, namely,

$$\frac{dF}{d\tau} = (\mathrm{Re}^* - \mathrm{Re}_c^*)F - F^3, \quad (4)$$

with $\mathrm{F}_\omega^y(t) = \alpha F(\tau)\sin t = \alpha\Im(F(\tau)e^{i(t-\pi/2)})$. In these expressions, the time τ (which is normalized by the scale t_0 instead of t_ω) is given by

$$\tau = \frac{\beta t}{S(\mathrm{Re}^* - \mathrm{Re}_c^*)}. \quad (5)$$

The prefactors α and β are adjustable. Here, we take $\alpha = 1/15$ and $\beta = 2/5$ to match the measurements of F_ω^y reported in [12]. Though (4) is reminiscent of a Landau equation, it is not meant here to describe the transition between the rectilinear and oscillatory paths of the body, since the nature of this transition is not clear for the time being: though the onset of path oscillations is very close to Re_c^* for thick bodies ($\chi \leq 6$), thin bodies exhibit path oscillations only for much larger Re^* [7]. In the case of axisymmetric bodies held fixed in a steady uniform flow, it has also recently been shown that the nature of the successive bifurcations in the wake depends on the body shape [15]. The precise modeling of the transition thus requires a specific effort, which is beyond the scope of the present Letter. Instead, the aim of Eq. (4) is to model the growth and saturation of the transverse force for the range of parameters corresponding to the zigzag regime. The most interesting point is that the length of the transient required for the body path to reach regular oscillations is inversely proportional to the Strouhal number for all bodies and therefore depends mostly on the aspect ratio χ and only weakly on Re^* (see below).

So far, the model incorporates information about the state of the wake, in particular its strength and rate of evolution, that depends on the mean rise motion of the body through the modified Reynolds number Re^* and the inertial time scale τ. The next step is to bring into play the

oscillatory degrees of freedom of the body. We note that the model should somehow encapsulate the case of a body held fixed in a steady uniform flow. However, the phase difference and the amplitude ratio between the vortical torque and the vortical transverse force depend strongly on the aspect ratio χ when the body is free to move, whereas they do not when it is fixed [12]. We therefore conjecture that the effect of the body degrees of freedom on the vortical loads must be expressed as a deviation from the behavior of fixed bodies. More precisely, we assume that the vortical torque is linked both to the vortical transverse force and to the body degrees of freedom as follows

$$\Gamma_\omega^z = l_d F_\omega^y(t + t_\Gamma) + \chi\Gamma_m(\theta, u, v, r, \ldots). \quad (6)$$

The first term corresponds to the torque already existing when the body is fixed. Numerical simulations for fixed bodies in a uniform flow (see [7] for technical details) showed that the phase difference t_Γ is small and that the lever arm l_d is in the range 0.15–0.2, increasing slightly with the aspect ratio. Here we choose $l_d = 0.19$ (i.e., the dimensional lever arm is $0.19d$) and $t_\Gamma = 0$ for simplicity and without significant effect on the results. The torque $\chi\Gamma_m$ is introduced to balance the differences in amplitude and phase observed when the body is free to move; these differences are larger when the body becomes thinner. Γ_m is expected to depend on the body kinematics, but since the vortical torque in (3) is known to be mainly balanced by the added-mass torque $(A - B)uv$ [12], we guess that Γ_m mainly depends on the rotational motion of the body. Figure 1 presents the amplitude and phase with respect to θ of Γ_m. It turns out that the amplitude, say Γ_m^{amp}, can be fitted as $\Gamma_m^{\text{amp}} = 5.3 \times 10^{-3}(\text{Re}^* - \text{Re}_c^*)^{1/2}$ and that the phase with respect to θ, say Φ, is nearly independent of χ for $\chi \geq 3$ and increases only slightly with Re^*, which leads to $\Phi = \frac{\pi}{180}(43.5 + 0.13(\text{Re}^* - \text{Re}_c^*))$. This suggests that Γ_m may be expressed as a combination of two terms: one in phase with the body inclination and one proportional to the body rotation r. We obtain

$$\Gamma_m = 0.09 \times (\gamma_1 \sin\theta - \gamma_2 r), \quad (7)$$

with $\gamma_1 = \cos\Phi$ and $\gamma_2 = \sin\Phi$, which are independent of χ. The first term can be thought of as a contribution

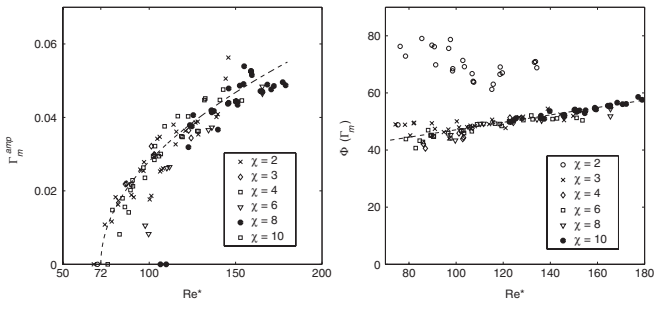

FIG. 1. Amplitude Γ_m^{amp} (left) and phase Φ (right) of the torque Γ_m as a function of χ and Re^* (experimental data from [12]). The dashed lines correspond to the fits.

resulting from the shift of the axial vortical force with respect to the body symmetry axis when the body inclines. Note that the prefactor χ in (6) indicates that the relevant length scale for the lever arm of this contribution is the body thickness h rather than d. In summary, our model for the vortical torque involves three contributions: two of them are the torques associated with the vortical transverse and axial forces acting off-centered on the body, while the third is due to the body rotation. The most remarkable point is that this model based on simple expressions allows us to describe accurately the vortical loads acting on the body for the whole range of parameters χ and Re^* covered in our experiments.

Nevertheless, the above expression for Γ_m implies that the vortical torque reacts immediately to a change in the body kinematics. It may instead seem more reasonable to assume that the instantaneous vortical torque depends on the past history of the body rotation since the latter influences the distribution of vortices in the wake. We therefore consider an alternative model for Γ_m involving an integro-differential operator of the body motion, namely,

$$\Gamma_m = -\gamma_0 \int_0^t e^{-\sigma(t-\tau)} \frac{dr}{d\tau} d\tau, \quad (8)$$

where $\gamma_0 = 0.12$ and $\sigma = \tan^{-1}\Phi$, which according to Fig. 1 implies that the time scale σ^{-1} is 3 to 6 times shorter than the period of the oscillations, depending on Re^*. Obviously $\Gamma_m = 0$ for a fixed body. Also (8) tends towards (7) at large time for periodic oscillations of r, since in this case $\gamma_0 = 0.09\sqrt{1 + \sigma^2} \simeq 0.12$. Expression (8) is consistent with the fact that the sign of the $\frac{dr}{dt}$ term in (3) is essentially opposite to that of Γ_ω^z, so that it does not appear as the response of the body to Γ_ω^z [12].

The system (2)–(6) supplemented by (7) or (8) can now be solved in terms of variables v, θ, r and F to compute the evolution of the body motion. For this purpose we employ a 4th-order Runge-Kutta algorithm. The initial conditions at $t = 0$ are $v = 0$, $\theta = 0$, $r = 0$ and $F = F_0$, corresponding to a body moving with a constant vertical velocity u on which a perturbation is introduced in the form of a transverse force F_0. Other sets of initial conditions could be used as well with no significant difference on the fully developed path. We also noticed that results obtained using (7) superimpose on those found using (8) within graphical accuracy. Figure 2 presents the computed inclination angle θ (solid lines) and the experimental measurements (dashed lines) for various values of χ and Re^*. In each case, a particular value of the initial perturbation F_0 is chosen to match the experimental growth of the amplitude of θ. Obviously, the magnitude of the perturbation also differs from one experimental case to another. Since the phase origin is also unknown in the experimental signal (when is the perturbation applied?), the phases are matched to coincide during the limit cycle. The curves show that the time required for each body to reach the constant-amplitude regime is well reproduced by the model. A similar agree-

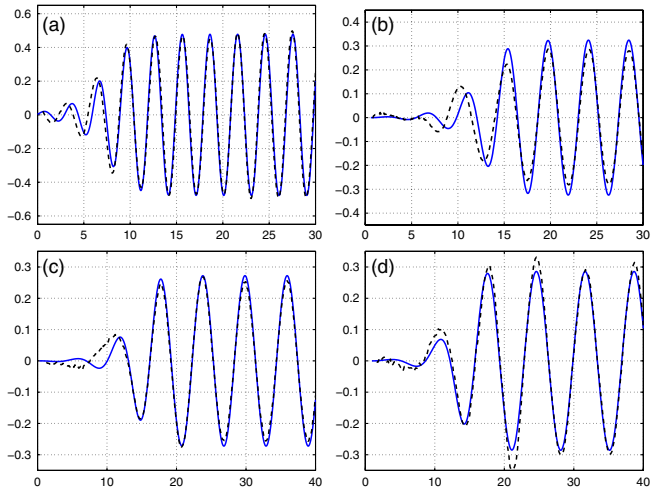

FIG. 2 (color online). Evolution of the computed (solid line) and experimental (dashed line) inclination angle θ for: (a) a thin body with $\chi = 10$, $\mathrm{Re}^* = 155$, $F_0 = 0.026$; (b) an intermediate body with $\chi = 6$, $\mathrm{Re}^* = 112$, $F_0 = 0.04$; (c) a thick body with $\chi = 3$, $\mathrm{Re}^* = 100$, $F_0 = -0.02$; (d) a thick body with $\chi = 2$, $\mathrm{Re}^* = 103.5$, $F_0 = 0.036$.

ment is obtained for the transverse velocity (not shown). Noticeably, Fig. 2 indicates that the behavior of a thick body with $\chi = 2$ can also be satisfactorily predicted by the model, despite the poor agreement on the phase Φ between the model and the experiments (Fig. 1). The diversity of body kinematics recovered by the model is illustrated in Fig. 3: the computed evolutions of θ (dashed lines) and v (solid lines) for a thin ($\chi = 10$) and a thick ($\chi = 3$) body exhibit contrasting relative amplitudes and phases, corresponding to the 2D plate-type and the bubble-type behavior, respectively.

The strength of the model presented in this Letter is twofold. First, it makes use of the generalized Kirchhoff equations supplemented by a nonlinear model of the vortical loads that incorporates several ingredients directly deduced from experiments. In particular this model is capable of reproducing accurately both the transient and the saturated state of the body motion. Second, and perhaps more importantly, it identifies two contributions in the vortical loads. The first of these, which already exists for fixed bodies, results from the shedding of vortices in the wake. The second arises from the feedback of the body degrees of freedom on the wake dynamics. Since these two contributions scale differently with χ, each of them required a specific modeling. The final model we obtained allows the oscillatory behavior of freely moving axisymmetric bodies such as disks and oblate spheroids to be reproduced quantitatively over a wide range of aspect ratios. In contrast, this model is valid over a limited range of Reynolds number since it only incorporates the physics of the first oscillating regime. Moreover, since the only nonlinearity in the model is that introduced in (4), highly

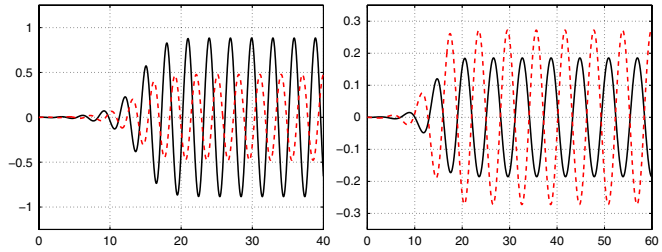

FIG. 3 (color online). Predicted evolutions of θ (dashed line) and v (solid line) for the thin body with $\chi = 10$ (left) and the thick body with $\chi = 3$ (right) of Fig. 2.

nonlinear body paths cannot be reproduced with this formulation. In particular the tumbling motion of [3] requires extra nonlinearities to be taken into account. The present model can be straightforwardly extended to certain classes of three-dimensional paths. In the absence of rotation of the body about its symmetry axis, a similar modeling for the additional vortical loads F_ω^z and Γ_ω^y can be introduced with appropriate coefficients. If a smaller value of α is used for F_ω^z, the model generates quasi-two-dimensional paths, like those observed in [7]. If a smaller value of β is employed for F_ω^z, zigzag paths evolving into helical paths, like those observed in the case of an oblate bubble [11], are obtained.

[1] L. Mahadevan, C.R. Acad. Sci. Paris **323**, 729 (1996).
[2] A. Belmonte, H. Eisenberg, and E. Moses, Phys. Rev. Lett. **81**, 345 (1998).
[3] U. Pesavento and Z. J. Wang, Phys. Rev. Lett. **93**, 144501 (2004).
[4] A. Andersen, U. Pesavento, and Z. Wang, J. Fluid Mech. **541**, 91 (2005).
[5] W. Shew and J.-F. Pinton, Phys. Rev. Lett. **97**, 144508 (2006).
[6] P. Fernandes, P. Ern, F. Risso, and J. Magnaudet, Phys. Fluids **17**, 098107 (2005).
[7] P. Fernandes, F. Risso, P. Ern, and J. Magnaudet, J. Fluid Mech. **573**, 479 (2007).
[8] P. Ern, P. Fernandes, F. Risso, and J. Magnaudet, Phys. Fluids **19**, 113302 (2007).
[9] H. Lamb, *Hydrodynamics* (Cambridge University Press, Cambridge, England, 1932), 6th ed.
[10] M. Howe, Q. J. Mech. Appl. Math. **48**, 401 (1995).
[11] G. Mougin and J. Magnaudet, Phys. Rev. Lett. **88**, 014502 (2001).
[12] P. Fernandes, P. Ern, F. Risso, and J. Magnaudet, J. Fluid Mech. **606**, 209 (2008).
[13] P. Albarede and P. Monkewitz, Phys. Fluids A **4**, 744 (1992).
[14] M. Facchinetti, E. de Langre, and F. Biolley, J. Fluids Struct. **19**, 123 (2004).
[15] D. Fabre, F. Auguste, and J. Magnaudet, Phys. Fluids **20**, 051702 (2008).